# Lateral Reliability Assessment of Eccentrically Braced Frames Including Horizontal and Vertical Links Under Seismic Loading

Fayçal Abdelhamid
LGC-ROI, Civil Engineering Laboratory - Risks and Structures Interactions, Faculty of Technology
University of Batna 2
Batna, Algeria
f.abdelhamid@univ-batna2.dz

Djarir Yahiaoui
LGC-ROI, Civil Engineering Laboratory - Risks and Structures Interactions, Faculty of Technology
University of Batna 2
Batna, Algeria
djarir.yahiaoui@univ-batna2.dz

Mohamed Saadi
LGC-ROI, Civil Engineering Laboratory - Risks and Structures Interactions, Faculty of Technology
University of Batna 2
Batna, Algeria
m.saadi@univ-batna2.dz

Noureddine Lahbari
LGC-ROI, Civil Engineering Laboratory - Risks and Structures Interactions, Faculty of Technology
University of Batna 2
Batna, Algeria
n.lahbari@univ-batna2.dz

*Received: 20 January 2022 | Accepted: 1 February 2022*

**Abstract-Eccentrically Braced Frames (EBFs) have been widely used in the last decades and proved their efficiency to resist strong earthquake intensities by providing suitable ductility and lateral stiffness. Using the PBPD method for the design, EBFs can fulfill the target performance objectives under major earthquakes. The most commonly used configurations are the K-shaped and the recent Y-shaped EBFs, which have the advantage that the links are independent of the beam and can be easily replaced after an earthquake without serious damage to the beam and slab. This study focused on the lateral reliability of both systems under seismic loading. Nonlinear static pushover and Incremental Dynamic Analysis (IDA) were performed on 5-story and 10-story K- and Y-shaped EBFs. A series of 14 near- and 7 far-field seismic records were considered to analyze and compare the inter-story drifts of both systems using the Seismostruct software. Moreover, Peak Ground Accelerations (PGA) and the different performance levels were also examined.**

***Keywords-eccentric braces; short links; incremental dynamic analysis; performance based design; interstory drift***

## I. INTRODUCTION

During the last 50 years, many studies have been carried out through experimental and numerical research with the aim of better understanding the behavior of Eccentrically Braced Frame (EBF) systems and developing adequate design methods to improve their performance against seismic and wind loads. This lateral load-resisting system, originated from Japan, combines the advantages of both Moment Resisting Frame (MRF) and Concentrically Braced Frame (CBF) by ensuring high elastic stiffness and energy dissipation during severe earthquakes. One of the most important key parameters that controls the behavior of EBF systems is the segment *e* between braces or brace to the column. This segment, called the link, acts as a structural fuse to dissipate the energy induced by earthquakes in a building. The remaining parts of the structure are designed to remain essentially elastic when links yield. The link length ratio $\rho$ is a function of *e*, plastic shear $V_p$, and plastic moment $M_p$ capacities of the link [$\rho=e/(M_p/V_p)$]. Depending on the length ratio ($\rho$), shear yielding controls the behavior of short links while flexural yielding is predominant in long links. The experimental research conducted in [1-4] showed that short links exhibit better performance under cyclic loadings in terms of ductility and strength. A link is classified as short if $\rho$<1.6, while links with $\rho$>2.6 are considered long. These practical limitations were proposed through experimental studies of various link specimens [3, 5-7] and were adopted by many design specifications, including AISC 341-10 [8]. The effect of adding stiffeners to improve the strength and energy dissipation capacity of links] to achieve a better performance of shear links and avoid web local buckling and strength degradation has been highlighted in [3, 9-10. Unlike shear links, stiffeners in long links may not prevent flange buckling but could limit strength degradation [11]. Intermediate stiffeners may be useful in flexural links if a significant axial force is acting on the link [12]. Various numerical modeling techniques of links were developed in [10, 13-14] to demonstrate their accuracy with experimental results. More recently, a simplified approach was presented in [15] by modeling elements with concentrated hinges at the ends. This approach has been used in numerical studies [16, 17]

Corresponding author: Fayçal Abdelhamid

highlighting some deficiencies in the cyclic response of links. In [18], the previous element model was improved using the uniaxial material model of Zona and Dall'Asta to define the responses of the flexural and shear hinges. The efficiency of this approach was highlighted by comparing numerical and test results. More element models have been developed to model steel links and members in the EBFs. The model developed in [19, 20] was improved in [21] by combining axial, shear, and flexural hinges in the elements to demonstrate the accuracy of the proposed approach. Alternative EBF systems were presented in [22] to improve the performance of structures by integrating a damping system to resist lateral loading. In [23], a linkage system was proposed that combined Pall friction and rotational friction damper to improve energy dissipation capacity.

In practical applications, systems with horizontal links (K-type) are the most commonly used because of their excellent performance during earthquakes. Systems with vertical links (Y-type) have also shown great cyclic performance in the experiments conducted in [24-26]. However, some deficiencies were observed at the conjunction of the vertical link and the braces due to significant out-of-plane deformations. The main goal of this study is to compare the lateral reliability of the EBF, including horizontal and vertical links, through nonlinear pushover and incremental dynamic analysis. For this purpose, 14 near-field and 7 far-field seismic records were selected to study the behavior of 5-story and 10-story EBF models. The parameter considered for the comparison of the two systems was the inter-story drift.

## II. NUMERICAL MODELING VERIFICATION STUDY

As a first step, model validation was carried out to ensure that numerical results could represent the behavior of EBFs under real conditions. To achieve this purpose, the experimental test conducted in [27] was used to build a numerical model using the Seismostruct 2021 software [28]. The specimen tested in [27] and compared with the numerical model was a single-story single-bay 1/2 scale Y-EBF made with high-strength steel. The height and width of the specimen were 1.8m and 3.6m respectively, while a short link with a length of 0.5m was used. Table I highlights the welded H-shaped sections and the materials of the specimen elements. A vertical load of 400kN was applied to the top of the column to simulate the axial force transferred to it by the superstructure. Monotonic loading and pseudostatic tests were performed at a loading speed of 0.05mm/s until structural failure [27].

TABLE I. SECTIONS AND MATERIALS OF THE SPECIMEN ELEMENTS

| Members | Sections | Material |
|---|---|---|
| Column | H150××150×6×10 | Q460 |
| Beam | H225×125×6×10 | Q460 |
| Link | H225×125×6×10 | Q345 |
| Brace | H125×120×6×10 | Q460 |

Based on the experimental data, a numerical model was developed using Seismostruct 2021 [28]. The element type defined in the numerical model for beam and column was the inelastic plastic-hinge force-based frame element "InfrmFBPH", where hinges were located at both ends of beam and column. An inelastic truss element was used for the braces, and an inelastic plastic hinge displacement-based frame element InfrmDBPH was assumed for the link, as shown in Figure 1. The software automatically assigns the fibers of the section at the element's end with a sufficient number to ensure an adequate reproduction of the stress-strain distribution across the cross-section of the member.

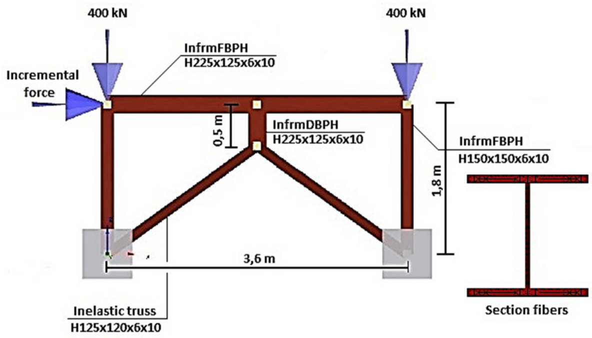


Fig. 1. The numerical model of the studied specimen.

The modeling parameters used for the link were selected according to tables 9-7 of the ASCE 41-17 standard [29]. A bilinear stress-strain steel model with kinematic strain hardening was also defined for elements with their corresponding property values.

Pushover analysis was performed by imposing an incremental force at the top of the column until the model failed. The resulting capacity curve was compared with the experimental test results obtained in [27]. The comparison of the experimental and the numerical results is shown in Figure 2. The ultimate base shear of the experimental test was approximately 680kN, while a value of 618kN was recorded in the simulation model. The results appear to agree with the experimental evaluation with a maximum relative error of 9%. Therefore, it can be concluded that numerical modeling is capable of simulating the response of the specimen with sufficient accuracy and can be used to predict the dynamic behavior of EBFs.

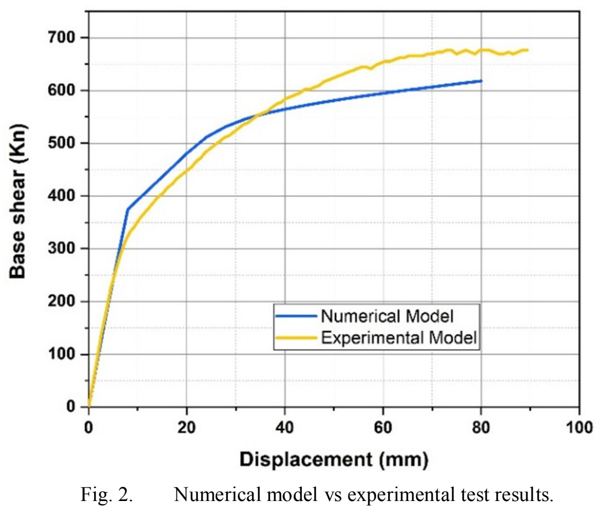


Fig. 2. Numerical model vs experimental test results.

## III. PUSHOVER AND INCREMENTAL DYNAMIC ANALYSIS

In [27], four groups of Y-type EBFs of 5, 10, 15, and 20 storeys were designed, using a performance-based seismic design method, according to the Chinese seismic code for buildings [30]. Ordinary and high-strength steel was used for each group to be compared in terms of bearing capacity, lateral stiffness, story drift, link rotation, and failure modes. The prototypes were characterized by a peak ground acceleration of 0.3g with a 10% probability of exceedance over 50 years. All frames had a typical story height of 3.6m, 3 bay spans of 7.2m, and a vertical link length of 0.8m. Welded H-sections were used for all frame members except for the column where box sections were assigned. Among the 8 designed Y-type EBFs, frames with 5 and 10 storeys made with ordinary steel (Q345) were investigated. Additional EBF models were also studied in parallel, including horizontal (K-type) instead of vertical links, using the same cross-sections and geometrical dimensions as the selected models to ensure a fair comparison. Pushover analysis was performed for all prototypes using the same member modeling parameters as for the verification model. Connections were considered rigid for all models. The material yield strength used for all the element members was the nominal value of ordinary steel Q345 ($f_y$=345MPa), and the elastic modulus was equal to 2.06×105MPa. The dead and live loads applied on the floor were 5.0kN/m² and 2.0kN/m², respectively. For the roof, the dead and live loads were 6.0kN/m² and 2.0kN/m². A snow load was also assigned to the roof with a value of 0.35kN/m² [27]. The fundamental periods obtained from the modal analysis of the investigated prototypes are shown in Table II, while the adopted sections for all members are presented in Tables III and IV. Incremental Dynamic Analysis (IDA) was also applied using a set of selected ground motion records from the PEER NGA database (14 near-field earthquakes and 7 far-field earthquakes), as recommended in FEMA695 [31]. Each earthquake represents a particular seismic intensity and is used multiple times at different scales so that the structure is subjected to a wide range of elastic and inelastic behavior. Tables V and VI highlight the ground motion records used in this analysis. The Newmark integration method was used with $\beta$=0.25 and $\gamma$=0.5. The IDA offers various advantages compared to the pushover analysis and has proved its accuracy by considering the effect of higher modes in the analysis [32-33].

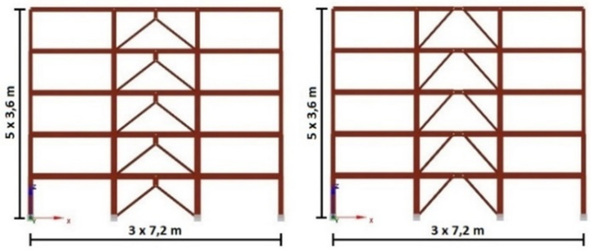


Fig. 3. 5-story Y-type and K-type prototypes.

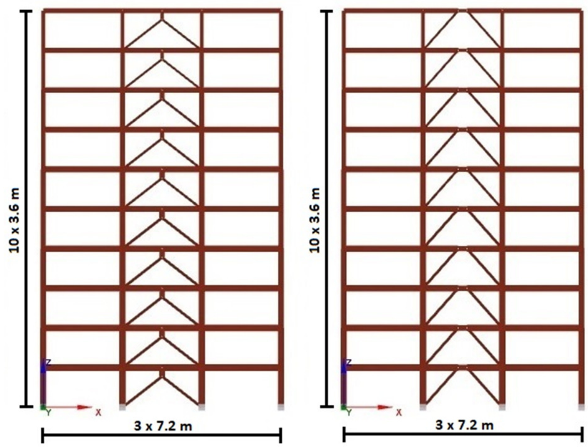


Fig. 4. 10-story Y-type and K-type prototypes.

TABLE II. FUNDAMENTAL PERIODS

| Models | T1 (s) | T2 (s) | T3 (s) |
|---|---|---|---|
| 5-story Y-type | 0.722 | 0.273 | 0.164 |
| 5-story K-type | 0.610 | 0.225 | 0.137 |
| 10-story Y-type | 1.296 | 0.465 | 0.270 |
| 10-story K-type | 1.191 | 0.415 | 0.231 |

TABLE III. 5-STORY EBF MEMBER SECTIONS

| Story | Beam | Link | Column with brace | Column with no brace | Brace |
|---|---|---|---|---|---|
| 5 | H410×150×6×10 | H330×150×4×10 | 400×400×16 | 300×300×12 | H200×200×8×12 |
| 4 | H440×150×10×16 | H420×180×6×10 | 450×450×18 | 350×350×16 | H200×200×10×16 |
| 3 | H490×180×10×16 | H410×180×8×12 | 500×500×18 | 350×350×16 | H200×200×10×16 |
| 2 | H520×200×10×16 | H470×180×8×12 | 550×550×20 | 400×400×18 | H220×220×10×16 |
| 1 | H550×200×10×16 | H500×180×8×12 | 550×550×20 | 450×450×18 | H220×220×10×16 |

TABLE IV. 10-STORY EBF MEMBER SECTIONS

| Story | Beam | Link | Column with brace | Column with no brace | Brace |
|---|---|---|---|---|---|
| 10 | H440×160×6×10 | H320×140×5×10 | 350×350×16 | 350×350×12 | H200×200×10×16 |
| 9 | H480×200×8×12 | H310×150×8×14 | 400×400×16 | 350×350×12 | H200×200×10×16 |
| 8 | H490×200×10×16 | H430×180×8×14 | 450×450×18 | 400×400×16 | H220×220×10×16 |
| 7 | H530×220×10×16 | H420×200×10×16 | 450×450×20 | 400×400×16 | H220×220×10×16 |
| 6 | H560×240×10×16 | H470×200×10×16 | 500×500×20 | 450×450×18 | H220×220×10×16 |
| 5 | H540×240×12×18 | H510×200×10×16 | 500×500×20 | 450×450×18 | H250×250×10×16 |
| 4 | H570×240×12×18 | H470×200×12×18 | 550×550×22 | 500×500×20 | H250×250×10×16 |
| 3 | H590×240×12×18 | H490×200×12×18 | 550×550×22 | 500×500×20 | H250×250×10×16 |
| 2 | H610×240×12×18 | H510×200×12×18 | 600×600×25 | 550×550×20 | H250×250×10×16 |
| 1 | H620×240×12×18 | H520×200×12×18 | 600×600×25 | 550×550×20 | H250×250×10×16 |

TABLE V. NEAR-FIELD GROUND MOTION RECORDS

| Earthquake Name | Year | Station Name | Magnitude | Rjb (km) |
|---|---|---|---|---|
| Cape Mendocino | 1992 | Petrolia | 7.0 | 9.5 |
| Darfield_ New Zealand | 2010 | TPLC | 7.0 | 6.11 |
| Duzce_ Turkey | 1999 | Lamont 1062 | 7.1 | 9.14 |
| Erzincan_ Turkey | 1992 | Erzincan | 6.7 | 2.0 |
| Gazli_ USSR | 1976 | Karakyr | 6.8 | 3.92 |
| Imperial Valley-06 | 1979 | Chihuahua | 6.5 | 7.29 |
| Irpinia_ Italy-01 | 1980 | Sturno (STN) | 6.9 | 6.78 |
| Kobe_ Japan | 1995 | Port Island | 6.9 | 3.31 |
| Kocaeli_ Turkey | 1999 | Yarimca | 7.5 | 1.38 |
| Loma Prieta | 1989 | Saratoga - Aloha Ave | 6.9 | 7.58 |
| Nahanni_ Canada | 1985 | Site 1 | 6.9 | 2.48 |
| Niigata_ Japan | 2004 | NIG017 | 6.8 | 4.22 |
| Northridge-01 | 1994 | N Hollywood - Coldwater Can | 6.7 | 7.89 |
| Superstition Hills-02 | 1987 | Superstition Mtn Camera | 6.5 | 5.61 |

TABLE VI. FAR-FIELD GROUND MOTION RECORDS.

| Earthquake Name | Year | Station Name | Magnitude | Rjb (km) |
|---|---|---|---|---|
| Imperial Valley-06 | 1979 | Delta | 6.5 | 22.03 |
| Irpinia_ Italy-01 | 1980 | Calitri | 6.9 | 13.34 |
| Loma Prieta | 1989 | Gilroy Array #4 | 7.0 | 13.81 |
| San Fernando | 1971 | LA-Hollywood Stor FF | 6.6 | 22.77 |
| Spitak_ Armenia | 1988 | Gukasian | 6.7 | 23.99 |
| Superstition Hills-02 | 1987 | Westmorland Fire Sta | 6.5 | 13.03 |
| Tabas_ Iran | 1978 | Boshrooyeh | 7.4 | 24.07 |

TABLE VII. LIMIT STATES OF EBF ACCORDING TO FEMA 356

| Limit states | Recommended drifts (%) |
|---|---|
| Immediate occupancy (IO) | 0.5 |
| Life safety (LS) | 1.5 |
| Collapse prevention (CP) | 2.0 |

The demand parameter considered was the inter-story drift ratio (maximum inter-story drift of all storeys). The performance levels and their corresponding drift values for EBF are presented in Table VII according to FEMA356 [34].

## IV. RESULTS AND DISCUSSION

The seismic reliability of EBFs having K-type and Y-type links was investigated using non-linear static pushover and incremental dynamic analysis on 5 and 10-story frames.

### *A. Pushover Analysis*

The EBFs with vertical links exhibited higher inter-story drifts, especially in the intermediate storeys. The difference was about 20% between the drift of the K and Y types for the 5-story model (maximum inter-story drift at the 3rd floor) and 53% for the 10-story model (maximum inter-story drift at the 5th floor). The inter-story drift is more significant as the height of the structure increases. The K-type system exhibited more important lateral stiffness than the Y-type system in all cases. According to [30], the link deformation reaches the plastic limit state when the drift value of the story exceeds 2%. The results, shown in Figure 5, indicate that the yielding of the links in the Y-type models has already occurred for the intermediate stories, while in the K-type models the links reach the plastic limit state.

### *B. Incremental Dynamic Analysis (IDA)*

A series of IDAs were performed on the selected EBF models to examine the performance of the K and Y types at different earthquake intensities and to evaluate the peak ground accelerations corresponding to each specific limit state of the structures. The maximum inter-story drift recorded for the 5 and 10-story studied prototypes under the 21 selected earthquakes are shown in Figures 6 and 7, where the Peak Ground Acceleration (PGA) was selected as the intensity measure, and the maximum inter-story drift ratio was selected as the response measure. The limit states IO, LS, and CP at 0.5, 1.5, and 2% respectively, are shown in Figures 6 and 7.

The results in Figure 7 show that the corresponding PGA for the different damage levels is higher for models with horizontal links (K-type). In the 5-story EBFs, a PGA of 0.73g was recorded for the K-type model against 0.4g for Y-type at the collapse prevention level. For the 10-story EBFs, the K-type model reached the limit of 2% drift ratio at a PGA of 0.5g while the Y-type model reached the same limit at 0.31g. To attain the collapse prevention performance level, the K-type systems required 1.7 times higher average intensity than the Y-type systems. It should be noted that as the height of the frame increases, the intensity that leads to the yielding of links decreases. This implies that shorter frames in general exhibit higher levels of reliability. The results in Figure 7 also show that the links in both systems produced intensities above the intensity corresponding to the design hazard level, that is 0.3g. Therefore, the performance-based seismic design method once again proved its efficiency in providing structures with good lateral stiffness to sustain subsequent earthquake intensities.

(a)

(b)

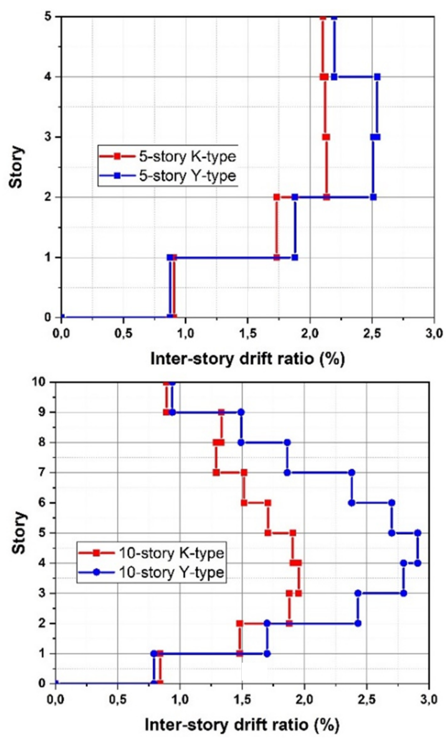


Fig. 5. Inter-story drift ratio at 2% target (a) 5-story (b) 10-story models.

(a)

(b)

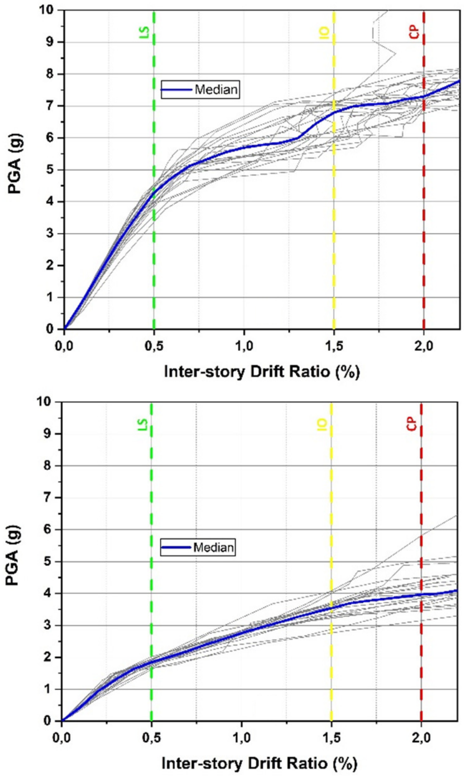


Fig. 6. IDA curves of 5-story models (a) K-type (b) Y-type.

(a)

(b)

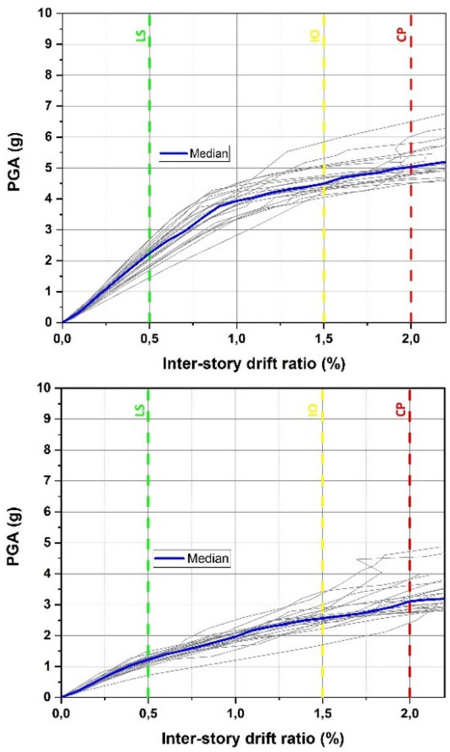


Fig. 7. IDA curves for 10-story models (a) K-type (b) Y-type.

A clear comparison between the median IDA curves of 5 and 10-story prototypes is shown in Figure 8.

(a)

(b)

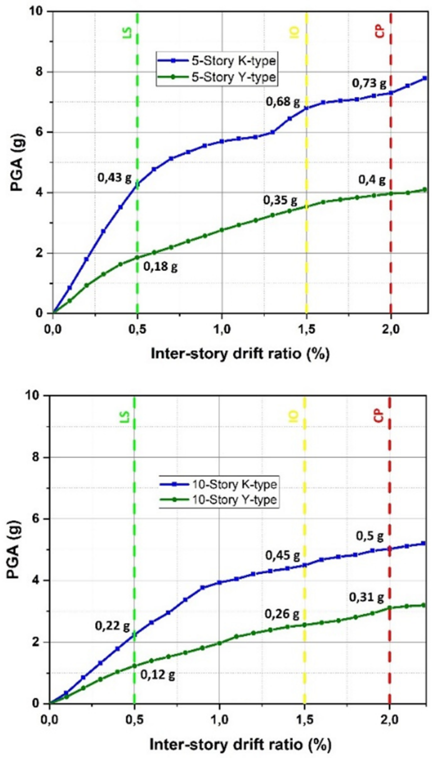


Fig. 8. Median IDA curves (a) 5-story models (b) 10-story models.

## V. CONCLUSIONS

This study investigated the lateral performance of EBFs including horizontal and vertical links. Modeling accuracy was examined using the Seismostruct software by comparing the modeling results with the experimental test conducted in [27]. The selected 5- and 10-story EBF models were analyzed using nonlinear pushover and incremental dynamic analysis over a series of 21 seismic records. The inter-story drifts obtained from the K- and Y-type EBF prototypes were compared under the same loading conditions. The following conclusions can be drawn:

- The results indicate that both K-type and Y-type systems can sustain major earthquake intensities and the links can meet the target performance objectives. However, the K-type system may absorb excessive seismic energy and provide better lateral stiffness by conferring smaller inter-story drifts to the structure compared to the Y-type system. The links in both systems start to yield in the intermediate floors but at different intensities (higher for the K-type models). Low-rise EBFs exhibit higher levels of reliability in general, where links reach the plastic limit state at higher intensities than the intensity corresponding to the design hazard level.
- With the same cross-sections, the K-type system exhibited better performance under the same loading conditions compared to the Y-type system. To achieve the same performance as the Y-type configuration, fewer cross-sections are needed for the K-type reducing the construction cost. However, links in the Y-type configuration can be

easily replaced after being damaged by an earthquake as they are not integrated with beams.

- The Performance-Based Seismic Design method (PBSD) demonstrated its efficiency in providing structures with sufficient lateral stiffness to resist major earthquake intensities. On the other hand, the numerical modeling with adequate parameters proved its ability to predict the dynamic behavior of EBFs with reasonable accuracy.

## REFERENCES

[1] C. W. Roeder and E. P. Popov, "Inelastic behavior of eccentrically braced steel frames under cyclic loadings," American Iron and Steel Institution, Washington, DC, USA, UCB/EERC-77/18, Dec. 1977.

[2] C. W. Roeder and E. P. Popov, "Cyclic Shear Yielding of Wide-Flange Beams," *Journal of the Engineering Mechanics Division*, vol. 104, no. 4, pp. 763–780, Aug. 1978, https://doi.org/10.1061/JMCEA3.0002378.

[3] K. D. Hjelmstad and E. P. Popov, "Seismic behavior of active beam links in eccentrically braced frames," National Science Foundation, Washington, DC, USA, UCB/EERC-83/15, Apr. 1983.

[4] K. D. Hjelmstad and E. P. Popov, "Cyclic Behavior and Design of Link Beams," *Journal of Structural Engineering*, vol. 109, no. 10, pp. 2387–2403, Oct. 1983, https://doi.org/10.1061/(ASCE)0733-9445(1983)109:10(2387).

[5] D. N. Manheim and E. P. Popov, "Plastic Shear Hinges in Steel Frames," *Journal of Structural Engineering*, vol. 109, no. 10, pp. 2404–2419, Oct. 1983, https://doi.org/10.1061/(ASCE)0733-9445(1983)109:10(2404).

[6] K. Kasai and E. P. Popov, "General Behavior of WF Steel Shear Link Beams," *Journal of Structural Engineering*, vol. 112, no. 2, pp. 362–382, Feb. 1986, https://doi.org/10.1061/(ASCE)0733-9445(1986)112:2(362).

[7] M. D. Engelhardt and E. P. Popov, "Behavior of Long Links in Eccentrically Braced Frames," American Iron and Steel Institution, Washington, DC, USA, UCB/EERC-89/01, Jan. 1989.

[8] "Seismic Provisions for Structural Steel Buildings," American Institure of Steel Construction, Chicago, IL, USA, ANSI/AISC Standard 341–10, 2010.

[9] J. O. Malley and E. P. Popov, "Design Considerations for Shear Links in Eccentrically Braced Frames," National Science Foundation, Washington, DC, USA, UCB/EERC-83/24, Nov. 1983.

[10] K. Kasai and E. P. Popov, "Cyclic Web Buckling Control for Shear Link Beams," *Journal of Structural Engineering*, vol. 112, no. 3, pp. 505–523, Mar. 1986, https://doi.org/10.1061/(ASCE)0733-9445(1986)112:3(505).

[11] M. D. Engelhardt and E. P. Popov, "Experimental Performance of Long Links in Eccentrically Braced Frames," *Journal of Structural Engineering*, vol. 118, no. 11, pp. 3067–3088, Nov. 1992, https://doi.org/10.1061/(ASCE)0733-9445(1992)118:11(3067).

[12] K. C. Tsai, Y. F. Yang, and J. L. Lin, "Seismic eccentrically braced frames," *The Structural Design of Tall Buildings*, vol. 2, no. 1, pp. 53–74, 1993, https://doi.org/10.1002/tal.4320020105.

[13] J. M. Ricles and E. P. Popov, "Dynamic Analysis of Seismically Resistant Eccentrically Braced Frames," American Iron and Steel Institution, Washington, DC, USA, UCB/EERC-87/07, Jun. 1987.

[14] J. M. Rides and E. P. Popov, "Inelastic Link Element for EBF Seismic Analysis," *Journal of Structural Engineering*, vol. 120, no. 2, pp. 441–463, Feb. 1994, https://doi.org/10.1061/(ASCE)0733-9445(1994)120:2(441).

[15] P. P. Rossi and A. Lombardo, "Influence of the link overstrength factor on the seismic behaviour of eccentrically braced frames," *Journal of Constructional Steel Research*, vol. 63, no. 11, pp. 1529–1545, Aug. 2007, https://doi.org/10.1016/j.jcsr.2007.01.006.

[16] M. Bosco, E. M. Marino, and P. P. Rossi, "Proposal of modifications to the design provisions of Eurocode 8 for buildings with split K eccentric braces," *Engineering Structures*, vol. 61, pp. 209–223, Nov. 2014, https://doi.org/10.1016/j.engstruct.2013.07.022.

[17] M. Bosco and P. P. Rossi, "A design procedure for dual eccentrically braced systems: Numerical investigation," *Journal of Constructional Steel Research*, vol. 80, pp. 453–464, Jan. 2013, https://doi.org/10.1016/j.jcsr.2012.08.003.

[18] M. Bosco, E. M. Marino, and P. P. Rossi, "Modelling of steel link beams of short, intermediate or long length," *Engineering Structures*, vol. 84, pp. 406–418, Oct. 2015, https://doi.org/10.1016/j.engstruct.2014.12.003.

[19] M. T. Kazemi, "Mixed Shear-Flexural (VM) Hinge Element and Its Applications," *Scientia Iranica*, vol. 14, no. 3, pp. 193–204, Jun. 2007.

[20] M. T. Kazemi and S. Erfani, "Special VM link element for modeling of shear–flexural interaction in frames," *The Structural Design of Tall and Special Buildings*, vol. 18, no. 2, pp. 119–135, 2009, https://doi.org/10.1002/tal.395.

[21] M. T. Kazemi and M. H. Asl, "Modeling of inelastic mixed hinge and its application in analysis of the frames with reduced beam section," *International Journal of Steel Structures*, vol. 11, no. 1, Feb. 2011, Art. no. 51, https://doi.org/10.1007/S13296-011-1005-7.

[22] N. W. Bishay-Girges, "An Alternative System for Eccentrically Braced Frames Resisting Lateral Loads," *Engineering, Technology & Applied Science Research*, vol. 9, no. 3, pp. 4281–4286, Jun. 2019, https://doi.org/10.48084/etasr.2778.

[23] G. Xu and M. Yamanari, "Performance of Steel Frame with Linkage System under Earthquake Excitation," *Engineering, Technology & Applied Science Research*, vol. 9, no. 1, pp. 3796–3802, Feb. 2019, https://doi.org/10.48084/etasr.2519.

[24] M. Seki, H. Katsumata, H. Uchida, and T. Takeda, "Seki, M., et al. "Study on earthquake response of two-storied steel frame with Y-shaped braces," in *Proceedings 9th world conference on earthquake engineering*, Tokyo-Kyoto, Japan, 1988, pp. 65–70.

[25] M. G. Vetr, "Seismic behavior, analysis and design of eccentrically braced frames with vertical shear links," Ph.D. dissertation, University of Technology Darmstadt, Germany, 1998.

[26] F. Wang, M. Su, M. Hong, Y. Guo, and S. Li, "Cyclic behaviour of Y-shaped eccentrically braced frames fabricated with high-strength steel composite," *Journal of Constructional Steel Research*, vol. 120, pp. 176–187, Dec. 2016, https://doi.org/10.1016/j.jcsr.2016.01.007.

[27] S. Li, Q. Wang, X. Li, and J. Tian, "Seismic performance of Y-type eccentrically braced frames combined with high-strength steel based on performance-based seismic design," *The Structural Design of Tall and Special Buildings*, vol. 29, no. 3, 2020, Art. no. e1689, https://doi.org/10.1002/tal.1689.

[28] Seismosoft, *SeismoStruct*. 2021.

[29] "Seismic Evaluation and Retrofit of Existing Buildings," American Society of Civil Engineers, ASCE/SEI 41-17, Dec. 2017, https://doi.org/10.1061/9780784414859.

[30] "GB 50011-2010 Code for Seismic Design of Buildings," Ministry of Housing and Urban-Rural Development of the People's Republic of China, Beijing, China, 2010.

[31] *Quantification of Building Seismic Performance Factors - FEMA P695*. Washington, DC, USA: U.S. Department of Homeland Security, FEMA, 2009.

[32] M. Javanpour and P. Zarfam, "Application of Incremental Dynamic Analysis (IDA) Method for Studying the Dynamic Behavior of Structures During Earthquakes," *Engineering, Technology & Applied Science Research*, vol. 7, no. 1, pp. 1338–1344, Feb. 2017, https://doi.org/10.48084/etasr.902.

[33] D. Vamvatsikos and C. A. Cornell, "Incremental dynamic analysis," *Earthquake Engineering & Structural Dynamics*, vol. 31, no. 3, pp. 491–514, 2002, https://doi.org/10.1002/eqe.141.

[34] "Prestandard and Commentary for the Seismic Rehabilitation of Buildings," American Society of Civil Engineers, Nov. 2000.